Artificial square ice and related dipolar nanoarrays

G. Möller[1] and R. Moessner[2]
[1] *Laboratoire de Physique Théorique et Modèles Statistiques, CNRS-UMR8626, 91406 Orsay, France and*
[2] *Laboratoire de Physique Théorique de l'Ecole Normale Supérieure, CNRS-UMR8549, Paris, France*
(Dated: April 4, 2006)

We study a frustrated dipolar array recently manufactured lithographically by Wang *et al.* [Nature **439**, 303 (2006)] in order to realize the square ice model in an artificial structure. We discuss models for thermodynamics and dynamics of this system. We show that an ice regime can be stabilized by small changes in the array geometry; a different magnetic state, kagome ice, can similarly be constructed. At low temperatures, the square ice regime is terminated by a thermodynamic ordering transition, which can be chosen to be ferro- or antiferromagnetic. We show that the arrays do not fully equilibrate experimentally, and identify a likely dynamical bottleneck.

Introduction: The ability to manipulate constituent degrees of freedom of condensed matter systems and their interactions is fundamental to attempts to advance our understanding of the variety of phenomena presented to us by nature. For a long time this has been achieved by utilizing the combinatorial richness of the periodic table of elements to construct different chemical compounds.

A more recent option is to use the tools of nanotechnology to custom-tailor degrees of freedom which can be assembled in a highly controlled manner; e.g. this has been proposed for realizing a topologically protected quantum computer using Josephson Junction arrays [2]. Submicron superconducting rings have also been used to provide effective spin-1/2 degrees of freedom [3].

Very recently, Wang and collaborators have used lithographic techniques to create a periodic two-dimensional array of single-domain submicron ferromagnetic islands [1], depicted in Fig. 1. This design approach takes advantage of well-established lithographic techniques and enables reading of the state of the system with local probes, such as magnetic force microscopes, to image the state of single constituent magnetic islands [4].

The first aim of this study is to assemble a system that realizes the square ice model. This is an attractive target model because of its long and distinguished history during which algebraic correlations and a finite entropy at zero temperature have been established, as well as connections to exact solutions, quantum magnetism, unusual dynamics and gauge theories [5].

The pioneering study by Wang *et al.* raises a number of important questions which we try to address here. Firstly, what are appropriate models for the arrays' thermodynamics and dynamics? Secondly, what other systems can one hope to build with these techniques? And thirdly, what are interesting directions in which further developments would be desirable?

In particular, the question of whether a dipolar system with long-range interactions can be modelled by the short-range ice model is rather similar to the one posed in the case of (three-dimensional) dipolar spin ice, where it was found that a nearest-neighbor description was surprisingly accurate for a range of properties, such as the low-temperature (Pauling) entropy [6–10].

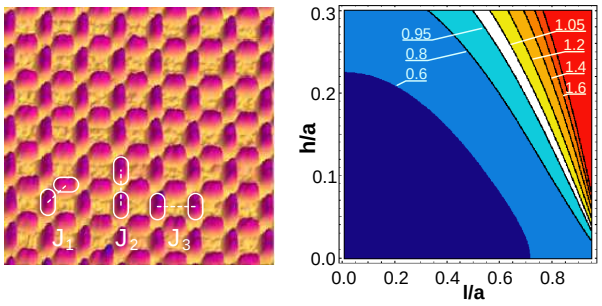

FIG. 1: (color online) Left: Atomic force microscope image of an array studied in Ref. 1. The islands have length $l = 220$nm, width 80nm and thickness 25nm. Right: Map of the ratio J_2/J_1 of the second to the first nearest neighbor interactions (highlighted in the left part) for different values of lattice constant, a, and sublattice height offset, h. Numbers indicate the ratio at the closest solid line. In the white zone, $|J_2/J_1 - 1| < 5\%$. In the left (blue) region, the ordered state is antiferromagnetic, whereas it is ferromagnetic in the right (yellow-red) area.

In this paper we show that an analogous equivalence between ice states and the ground states of two-dimensional dipoles on the links of the square lattice is more delicate. However, it can be established via a route quite different from the three-dimensional case, namely by (a) placing the dipoles pointing in different directions onto slightly different heights and (b) manufacturing the dipoles as elongated as possible. It turns out to be easier to realize kagome ice in a dipolar array, as the requisite symmetry is compatible with embedding in a plane.

As a byproduct, the low-temperature antiferromagnetic (in ice language: antiferroelectric) instability of the original model can be designed to be replaced by a ferromagnetic one. However, the experiments observe no ordering transition, implying that the array does not fully equilibrate. We are thus led to study a phenomenological model for its dynamics: zero-temperature ('greedy') stochastic dynamics subject to an energy barrier for spin flips. This reproduces the experimental measurements semi-quantitatively. Such dynamics are insufficient to an-

neal out isolated defects violating the ice rules even for strong interactions, thus preventing the establishment of an ice – or indeed an ordered – configuration.

In the remainder of this paper, we first analyze – by a mean-field theory and using Monte-Carlo simulations – the equilibrium statistical mechanics of arrays designed to mimic square and kagome ice. We then turn our attention to the dynamics of the arrays studied in Ref. 1 and present our results for the local correlations. We conclude with a brief discussion of disorder and an outlook.

Dipoles on the links of a square lattice: The interactions between the magnetic islands are dipolar, and therefore essentially a geometric property of the array (lattice constant: a), described by the Hamiltonian

$$H = \iint d\vec{r}_i d\vec{r}_j \frac{\vec{\mu}(\vec{r}_i)\cdot\vec{\mu}(\vec{r}_j) - 3[\vec{\mu}(\vec{r}_i)\cdot\hat{r}_{ij}][\vec{\mu}(\vec{r}_j)\cdot\hat{r}_{ij}]}{r_{ij}^3}, \quad (1)$$

where $\vec{r}_{ij} = \vec{r}_i - \vec{r}_j$, and $\vec{\mu}(\vec{r}_i)$ is the dipole moment at $\vec{r}_i$, which points along the link. We treat the dipoles either as points ($l/a \to 0$) or as uniform, monodomain needles of finite length l.

Can such an arrangement be used to access square ice physics? In other words, is there a (low-temperature) regime for such a dipolar system, where configurations obeying the ice rule are overwhelmingly present with approximately equal weights?

This is, by construction, the case for the 'Ising-ice model', in which the four islands emanating from a given vertex of the square lattice interact equally and antiferromagnetically, so that in the ground state two dipoles point into each vertex, and two out. These are precisely the ice states. The Fourier transform of this interaction has two branches (as there are two sites in the unit cell, one for each link direction of the square lattice), which have eigenvalues

$$\tilde{J}_l(q) = 0 \quad ; \tilde{J}_u(q) = 2J\left(\sin^2\frac{q_x}{2} + \sin^2\frac{q_y}{2}\right). \quad (2)$$

It is the flatness of the lower branch that indicates the frustration of the ice model. As all the ice states are linear combinations of the flat-band eigenvectors only, a sufficient condition for Eq. 1 to yield an ice regime is that its lower branch be flat and share the eigenvectors of the Ising-ice model [10], at least approximately.

By contrast, for a nearest-neighbor interaction only, one obtains a symmetric pair of bands:

$$J_{l,u}(q) = \pm 2J\left|\sin\frac{q_x}{2}\sin\frac{q_y}{2}\right|. \quad (3)$$

The spectrum for artificial ice (Fig. 2) lies in between, with a substantial dispersion to the flat 'ice' band, of about a third of the total bandwidth. Thus, there is a thermodynamic transition to antiferromagnetic order, which in our Monte-Carlo simulations occurs at temperature $T_{\rm af} = 1.68(4)J_1$ (where J_n is the strength of the $n^{\rm th}$-neighbor interaction, see examples in Fig. 1).

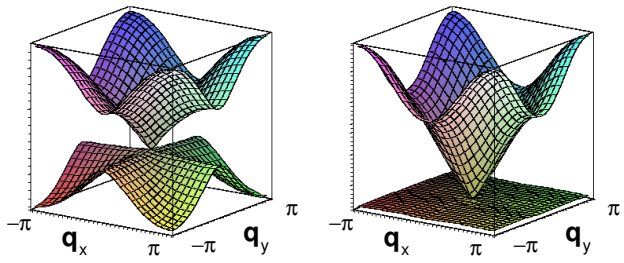

FIG. 2: (color online) Left: Spectrum for artificial ice (cut off after $10a$, for point-like dipoles). Right: same for $l/a = 0.7$ and $h/a = 0.207$: the lower band becomes almost flat, (less than 1.5% of the total bandwidth).

The principal reason for the dispersion of the lower band is the inequivalence – as in the F-model – of the six vertices of the ice model, which fall into two groups. One pair (labelled Type I in Ref. 1, see Fig. 3) has zero total magnetic moment, while the others (Type II) have a net moment along a diagonal and are higher in energy. This inequivalence results from the fact that, unlike the case of a tetrahedron in $d = 3$, the six bonds between the four islands belonging to a vertex are not all equivalent.

However, this can be remedied by introducing a height displacement h between magnetic islands pointing in the x- and y-directions.

The ratio J_2/J_1 of the two inequivalent bond energies (Eq. 1) is shown in Fig. 1 as a function of h/a and l/a. There is a set of choices for these parameters such that the interaction energies are approximately equal. For point-like dipoles ($l/a \to 0$), this value is

$$h_{\rm ice}/a = \sqrt{\left(\frac{3}{8}\right)^{2/5} - \frac{1}{2}} \approx 0.419\,, \quad (4)$$

and taking into account the finite extension of the dipoles lowers the required height offset. For instance, for $l/a = 0.7$, $h_{\rm ice}/a \approx 0.207$. In principle, for $1 - l/a \equiv \epsilon \to 0$, $h_{\rm ice}/a \sim \sqrt{2\epsilon} \to 0$. However, in this ideal limit the effects of disorder, finite transverse width and a possible internal structure of the dipoles will all play a role.

Having fixed the short-distance trouble by introducing the modulation in height, the question remains what happens to the long-distance part of the dipolar interaction, which in $d = 3$, amazingly, turned out to leave the ice regime intact [7, 9]. However, the mechanism responsible for this equivalence in $d = 3$ [10] is not operational in $d = 2$, as it requires the dimensionality of the dipolar interaction to coincide with that of the underlying lattice. Here, however, we have a $d = 3$, $1/r^3$ dipolar interaction in a $d = 2$ array. Nonetheless, the present situation is relatively benign, as the Fourier sum of a $1/r^3$ interaction in $d = 2$ is absolutely convergent (obviating the need for an Ewald sum).

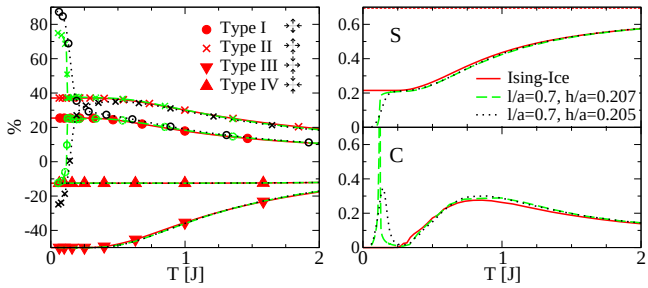

FIG. 3: (color online) Ising-ice vs. dipolar arrays: frequency of vertex types (% deviation from random distribution for single vertex, which is $\frac{1}{8}$, $\frac{1}{4}$, $\frac{1}{2}$ and $\frac{1}{8}$ for Types I-IV, respectively), entropy (S), and heat capacity (C) from Monte-Carlo simulations; x-axes were scaled for high-T asymptotics to coincide. The fraction of non-ice-rule vertices is below 1% for $T < 0.42J$ for all depicted systems. At low T, the ice regime, which widens with increasing l/a, is terminated by ferro- (dashed) or antiferromagnetic (dots) order for different h.

Further neighbor terms can be suppressed parametrically in the ideal limit of $l/a \to 1$. The ratio $J_{n\geq 3}/J_{1,2}$ vanishes as $\epsilon \to 0$, thus yielding the ideal Ising-ice model. As l/a is reduced, the flat band initially acquires only a small dispersion. To demonstrate this, in Fig. 2 we have plotted the mode spectrum for $l/a = 0.7$, which corresponds to the $a = 320$nm sample [1]. The overlap of its eigenvectors with those of the Ising-ice model differs from 1 by less than 0.1% over the entire Brillouin zone.

This demonstrates that an ice regime can be obtained by this route. Our Monte-Carlo simulations on the dipolar and the Ising-ice model for $l/a = 0.7$ (Fig. 3) bear out this statement: the intermediate ice regime is terminated at high T by thermally activated defects violating the ice rules, and at low T by an ordering transition. Choosing h on either side of the optimal value $h_{\rm ice}$, this transition is ferro/antiferromagnetic, respectively, and perhaps even to a more complicated state very close to $h_{\rm ice}$.

Kagome ice: The ground states of antiferromagnetic Ising spins on the kagome lattice define what is known as kagome ice, with the 'ice rules' requiring each triangle to have one spin pointing in and two out, or vice versa [11]. Since the sites of the kagome lattice correspond to the links of the honeycomb lattice, one can pose the question whether a dipolar array forming a honeycomb lattice will display a kagome ice regime.

The case of kagome ice has the advantage that the three bonds of the triangle are equivalent, unlike the six bonds of the square. This means that the nearest-neighbor Hamiltonian does not require any fine-tuning through a height offset. Furthermore, using the above limit of $\epsilon \to 0$, we can again parametrically suppress the importance of further-neighbor interactions, and hence obtain a representation of kagome ice. The vestiges of the further-neighbor terms will again give rise to an ordering transition, terminating the ice phase on its low-T side. We note that kagome ice is a phase distinct from square ice in that its long-wavelength theory is different – its correlations are not algebraic, but exponentially short-ranged even at zero temperature.

Dynamics and annealing: Given the impossibility of thermally equilibrating the array, the authors of Ref. 1 used a rotating magnetic field $B_{\rm ext}$, gradually stepped down, to speed up the dynamics [12]. The question whether such an 'algorithm' can be efficiently used to find the ground state of a system has been discussed in the context of spin glasses [13]. (However, in the case of an ice regime, the question is somewhat simpler, namely whether it is possible to find one of *exponentially* many ice configurations.)

For our model of dipolar needles, the energy scales for the arrays studied in Ref. 1 are:

$$\begin{aligned} \text{'Zeeman' energy}: &\quad |\mu \cdot B_{\rm ext}| \leq 2.6 \times 10^6 \text{K} \\ \text{'Exchange'}: &\quad 3.6 \times 10^3 \text{K} \leq J_1 \leq 1.1 \times 10^5 \text{K} \end{aligned} \tag{5}$$

Antiferromagnetic long-range order should thus be present at room temperature.

We consider a phenomenological model for the dynamics, motivated by the experimental protocol. Firstly, with the experimental temperatures well below the interaction strengths, we use a form of zero-temperature Monte-Carlo dynamics. Secondly, we note that vertices violating the ice rules are experimentally present throughout. As such defect vertices can be removed using single spin flips only, we impose a constraint on our single-spin-flip dynamics: for a flip to be accepted the energy gain must be above a threshold θ. Thirdly, the rotating field is modeled by a field of random orientation.

This model has two free parameters: the threshold θ and the speed with which the field is ramped down κ. We fix these parameters to be the same for all arrays, and fit them to obtain the best agreement with the experimental measurements of the local correlations (longer-range correlations in the experiment are very weak) [1]. The best fit is obtained for $\theta = 2.3 \times 10^5$ Kelvin and $\kappa = 87$ Tesla^{-1} attempted flips per spin during ramp-down (Fig. 4).

This algorithm gives semi-quantitative agreement with experiment over a range of interaction energies differing by a factor 30 (Eq. 5). However, we systematically overestimate the frequency of Type I vertices compared to those of Type II (as do other algorithms we have studied). This appears to be due to our needle model (Eq. 1) overestimating the ratio J_1/J_2. Denoting $\mathcal{E}_{ij} = \frac{E_i - E_I}{E_j - E_I}$, where E_i is the energy of an isolated Type i vertex, Ref. 1 finds from a finite-element simulation: $\mathcal{E}_{32} > 2$, $\mathcal{E}_{42} > 6$ for $l/a = 0.7$. If we reduce the value of $|J_1 - J_2|$ from Eq. 1 by 30%, our values grow from $\mathcal{E}_{32} = 1.7$, $\mathcal{E}_{42} = 4.9$, to 2.25 and 7, respectively. The resulting fit (Fig. 4, dashed lines) appears noise-limited [14].

Even for the strongest interactions, about 25% (non-ice-rule) defects, Type III vertices, persist. Whereas it is

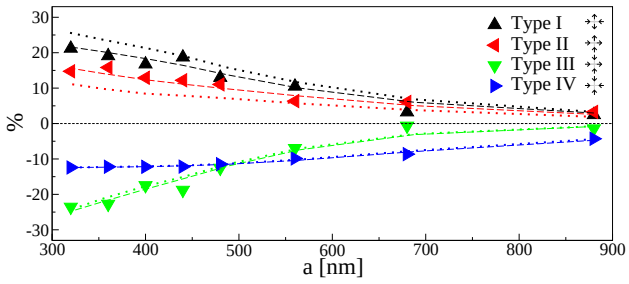

FIG. 4: (color online) Frequency of vertex types (as in Fig. 3). Interaction energies scale approximately as $1/a^3$, a factor of 30 between the extremal points. Experiments (symbols) are shown against dynamics simulations for needle dipoles (Eq. 1, dotted), and for increased J_2 (dashed, see text).

easy to remove pairs of appropriately oriented neighboring defects by flipping the spin which joins them, such an annihilation process occurs with low probability once these defects are sparse: they first need to diffuse around until they encounter a partner.

Disorder: Our dynamical model does not take into account disorder, which is expected to have substantial influence on the dynamical behavior even of single islands [4]. Thus, the good agreement of our model with the experiment might be due to its correct reproduction of the dynamical bottleneck, and not the detailed microscopic dynamics: the inability of the defects to 'find' one another may simply be due to their becoming pinned.

Disorder also impacts the ice regime thermodynamically, as the size of the leading perturbation sets the scale for its termination at low temperature. Especially for fine-tuned $h \sim h_{\rm ice}$, disorder might dominate (over $J_1 \neq J_2$ and further-neighbor interactions), by selecting some ice configurations over others; strong disorder might even lead to the presence of defects at any temperature.

To push the analysis further in this direction, experimental input would be desirable. What is the variance of the islands' geometrical properties? Are there some islands that freeze at much higher fields than others? Are defects usually located at the same positions, and what is their spatial distribution? How do correlations evolve during the ramp-down of the external field?

Summary and outlook: We have presented models for the dynamics and thermodynamics of frustrated dipolar arrays, including ways of stabilizing ice regimes. Perhaps the most interesting direction of further study involves their dynamics, in the presence of varying degrees of disorder. In particular, can other protocols [13], e.g. involving the use of AC magnetic fields, be used to speed up the dynamics? Note that in present samples, the largest interaction energies are more than two orders of magnitude above room temperature, so that further miniaturization is possible without resorting to cryogenics.

Better equilibration might then open the door for an experimental study of constrained classical [15] and perhaps eventually even quantum dynamics [3] (and quantum ice [16]). Even though this will require a substantial experimental effort, there appears to be no fundamental obstacle to obtaining at least a classical ice regime.

The results obtained along the way should provide insights into how the physics of frustration can lead to new ways of effectively suppressing interactions between neighboring magnetic nanoislands and into the limits imposed by disorder, a topic of interest with view to applications in memory storage [4]. We are thus optimistic that dipolar nanoarrays will provide an interesting field for further studies.

Acknowledgements: We thank P. Schiffer for several very helpful explanations and for assistance with the figures, and C. Henley, A. Middleton, S. Sondhi and O. Tchernyshyov for useful discussions. Some of our simulations made use of the ALPS library [17]. This work was in part supported by the Ministère de la Recherche et des Nouvelles Technologies with an ACI grant.

[1] R. F. Wang, C. Nisoli, R. S. Freitas, J. Li, W. McConville, B. J. Cooley, M. S. Lund, N. Samarth, C. Leighton, V. H. Crespi and P. Schiffer, Nature **439**, 303 (2006).
[2] L. B. Ioffe, M. V. Feigel'man, A. Ioselevich, D. Ivanov, M. Troyer and G. Blatter, Nature **415**, 503 (2002) .
[3] D. Davidovic, S. Kumar, D. H. Reich, J. Siegel, S. B. Field, R. C. Tiberio, R. Hey and K. Ploog, Phys. Rev. Lett. **76**, 815 (1996) ; H. Hilgenkamp, Ariando, H.-J. H. Smilde, D. H. A. Blank, G. Rijnders, H. Rogalla, J. R. Kirtley and C. C. Tsuei, Nature **422**, 50 (2003) .
[4] For a review, see J. I. Martín, J. Nogués, K. Liu, J. L. Vicent and I. K. Schuller, J. Mag. and Mag. Mat. **256**, 449 (2003) .
[5] E. H. Lieb, Phys. Rev. Lett. **18**, 692 (1967) and references thereof.
[6] S. T. Bramwell, Nature **439**, 273 (2006).
[7] R. Siddharthan, B. S. Shastry, and A. P. Ramirez, Phys. Rev. B **63**, 184412 (2001) .
[8] S. T. Bramwell, M. J. P. Gingras, Science **294**, 1495 (2001) .
[9] R. G. Melko, B. C. den Hertog and M. J. P. Gingras, Phys. Rev. Lett. **87**, 067203 (2001) .
[10] S. V. Isakov, R. Moessner and S. L. Sondhi, Phys. Rev. Lett. **95**, 217201 (2005) .
[11] A. S. Wills, R. Ballou and C. Lacroix, Phys. Rev. B **66**, 144407 (2002) .
[12] R. P. Cowburn, Phys. Rev. B **65**, 092409 (2002) .
[13] G. Zarand, F. Pazmandi, K. F. Pal and G. T. Zimanyi, Phys. Rev. Lett. **89**, 150201 (2002) .
[14] Such a change *reduces* the height offset, $h_{\rm ice}$, required to obtain equality of J_1 and J_2.
[15] D. Das, J. Kondev and B. Chakraborty, Europhys. Lett. **61**, 506 (2003) .
[16] R. Moessner, O. Tchernyshyov and S. L. Sondhi, J. Stat. Phys. **115**, 1769 (2004) .
[17] F. Alet *et al.*, J. Phys. Soc. Jap. Suppl. **74**, 30 (2005); M. Troyer, B. Ammon and E. Heeb, Lect. Notes Comput. Sci. **1505**, 191 (1998). See http://alps.comp-phys.org/.